

Chapter 15

Electrostatics

Electrostatic interactions are very important in molecular physics. Bio-molecules are usually embedded in an environment which is polarizable and contains mobile charges (Na^+ , K^+ , Mg^{2+} , $Cl^- \dots$). From a combination of the basic equations of electrostatics

$$\operatorname{div} D(\mathbf{r}) = \rho(\mathbf{r}) \quad (15.1)$$

$$D(\mathbf{r}) = \varepsilon(\mathbf{r})E(\mathbf{r}) \quad (15.2)$$

$$E(\mathbf{r}) = -\operatorname{grad} \Phi(\mathbf{r}) \quad (15.3)$$

the generalized Poisson equation is obtained

$$\operatorname{div}(\varepsilon(\mathbf{r}) \operatorname{grad} \Phi(\mathbf{r})) = -\rho(\mathbf{r}) = -\rho_{\text{fix}}(\mathbf{r}) - \rho_{\text{mobile}}(\mathbf{r}), \quad (15.4)$$

where the charge density is formally divided into a fixed and a mobile part

$$\rho(\mathbf{r}) = \rho_{\text{fix}}(\mathbf{r}) + \rho_{\text{mobile}}(\mathbf{r}). \quad (15.5)$$

Our goal is to calculate the potential $\Phi(\mathbf{r})$ together with the density of mobile charges in a self-consistent way.

15.1 Poisson Equation

We start with the simple case of a dielectric medium without mobile charges and solve (15.5) numerically.

15.1.1 Homogeneous Dielectric Medium

If ε is constant (15.5) simplifies to the Poisson equation

$$\Delta \Phi = -\frac{\rho}{\varepsilon}. \quad (15.6)$$

We make use of the discretized Laplace operator

$$\Delta f = \frac{1}{h^2} \{f(x+h, y, z) + f(x-h, y, z) + f(x, y+h, z) + f(x, y-h, z) + f(x, y, z+h) + f(x, y, z-h) - 6f(x, y, z)\} + O(h^2). \quad (15.7)$$

The integration volume is divided into small cubes which are centered at the grid points

$$\mathbf{r}_{ijk} = (hi, hj, hk). \quad (15.8)$$

The discretized Poisson equation averages over the six neighboring cells ($d\mathbf{r}_1 = (h, 0, 0)$, etc.):

$$\frac{1}{h^2} \sum_{s=1}^6 (\Phi(\mathbf{r}_{ijk} + d\mathbf{r}_s) - \Phi(\mathbf{r}_{ijk})) = -\frac{Q_{ijk}}{\varepsilon h^3}, \quad (15.9)$$

where $Q_{ijk} = \rho(\mathbf{r}_{ijk})h^3$ is the total charge in a cell. Equation (15.9) is a system of linear equations with very large dimension (for a grid with $100 \times 100 \times 100$ points the dimension of the matrix is $10^6 \times 10^6$!). We use the iterative method (Sect. 5.5)

$$\Phi^{\text{new}}(\mathbf{r}_{ijk}) = \frac{1}{6} \left(\sum \Phi^{\text{old}}(\mathbf{r}_{ijk} + d\mathbf{r}_s) + \frac{Q_{ijk}}{\varepsilon h} \right). \quad (15.10)$$

The Jacobi method ((5.88) on page 57) makes all the changes in one step whereas the Gauss–Seidel method ((5.91) on page 58) makes one change after the other. The chessboard (or black red method) divides the grid into two subgrids (with $i + j + k$ even or odd) which are treated subsequently. The vector $d\mathbf{r}_s$ connects points of different subgrids. Therefore it is not necessary to store intermediate values like for the Gauss–Seidel method. Convergence can be improved with the method of successive over-relaxation (SOR, (5.95) on page 59) using a mixture of old and new values

$$\Phi^{\text{new}}(\mathbf{r}_{ijk}) = (1 - \omega)\Phi^{\text{old}}(\mathbf{r}_{ijk}) + \omega \frac{1}{6} \left(\sum \Phi^{\text{old}}(\mathbf{r}_{ijk} + d\mathbf{r}_s) + \frac{Q_{ijk}}{\varepsilon h} \right) \quad (15.11)$$

with the relaxation parameter ω . For $1 < \omega < 2$ convergence is faster than for $\omega = 1$. For a square grid with $N = M^2$ points the optimum value of the relaxation parameter is

$$\omega_{\text{opt}} \approx \frac{2}{1 + \frac{\pi}{\sqrt{M}}}. \quad (15.12)$$

Convergence can be further improved by multigrid methods [75, 76]. Error components with short wavelengths are strongly damped during few iterations whereas it

takes a very large number of iterations to remove the long-wavelength components. But here a coarser grid is sufficient and reduces computing time. A small number of iterations give a first approximation f_1 with the finite residual

$$r_1 = \nabla^2 f_1 + \rho. \quad (15.13)$$

Then more iterations on a coarser grid are made to solve the equation

$$\nabla^2 f = -r_1 = -\rho - \nabla^2 f_1 \quad (15.14)$$

approximately. The residual of the approximation f_2 is

$$r_2 = \nabla^2 f_2 + r_1 \quad (15.15)$$

and the sum $f_1 + f_2$ gives an improved approximation to the solution since

$$\nabla^2(f_1 + f_2) = -\rho + r_1 + (r_2 - r_1) = -\rho + r_2. \quad (15.16)$$

This method can be extended to a hierarchy of many grids.

15.1.2 Charged Sphere

As a simple example we consider a sphere with a homogeneous charge density (Fig. 15.1)

$$\rho = e \frac{3}{4\pi R^3}. \quad (15.17)$$

The potential is given by

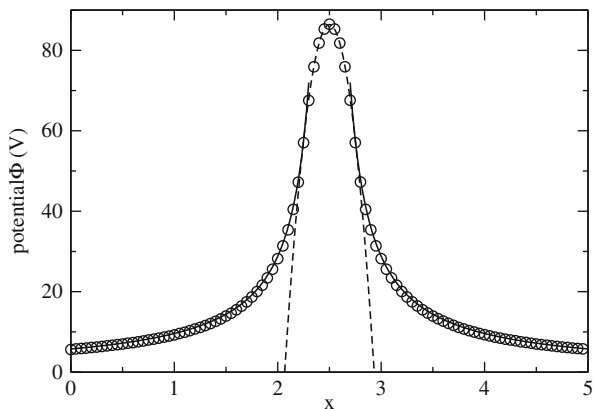


Fig. 15.1 Electrostatic potential of a charged sphere. A charged sphere is simulated with radius $R = 0.25 \text{ \AA}$ and a homogeneous charge density $\rho = e 3/4\pi R^3$ embedded in a dielectric medium. The grid consists of 100^3 points with a spacing of $h = 0.05 \text{ \AA}$. The calculated potential (circles) is compared to the exact solution ((15.18), curves)

$$\begin{aligned}\Phi(r) &= \frac{e}{4\pi\epsilon_0 R} + \frac{e}{8\pi\epsilon_0 R} \left(1 - \frac{r^2}{R^2}\right) \quad \text{for } r < R \\ \Phi(r) &= \frac{e}{4\pi\epsilon_0 r} \quad \text{for } r > R.\end{aligned}\tag{15.18}$$

Initial values as well as boundary values are taken from the potential of a point charge which is modified to take into account the finite size of the grid cells

$$\Phi_0(r) = \frac{e}{4\pi\epsilon_0(r+h)}.\tag{15.19}$$

The interaction energy is (Sect. 15.5) (Fig. 15.2)

$$E_{\text{int}} = \frac{1}{2} \int \varrho(\mathbf{r})\Phi(\mathbf{r})d^3r = \frac{3}{20} \frac{e^2}{\pi\epsilon_0 R}\tag{15.20}$$

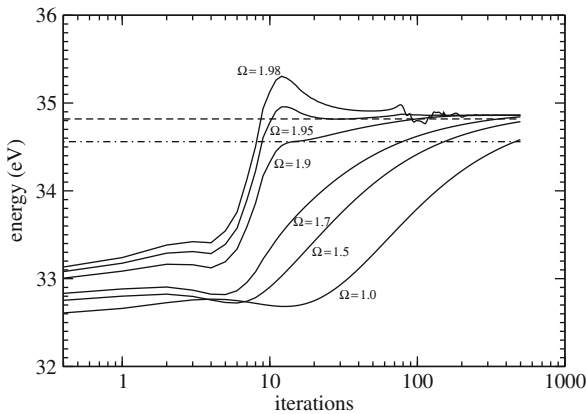


Fig. 15.2 Influence of the relaxation parameter. The convergence of the interaction energy ((15.20), which has a value of 34.56 eV for this example) is studied as a function of the relaxation parameter ω . The optimum value is around $\omega \approx 1.9$. For $\omega > 2$ there is no convergence. The *dash-dotted line* shows the exact value. The *dashed line* shows the exact radius which is derived from the occupied volume (15.35)

15.1.3 Variable ϵ

For variable ϵ we use the theorem of Gauss for a vector field \mathbf{F}

$$\int dV \operatorname{div}\mathbf{F} = \oint dA \mathbf{F}.\tag{15.21}$$

We choose $\mathbf{F} = \epsilon \operatorname{grad} \Phi$ and integrate over one cell

$$\int dV \operatorname{div}(\epsilon \operatorname{grad} \Phi) = \int dV (-\rho) = -Q_{ijk}\tag{15.22}$$

$$\oint dA \varepsilon \text{grad } \Phi = \sum_{\text{faces}} h^2 \varepsilon \text{grad } \Phi. \quad (15.23)$$

We approximate $\text{grad } \Phi$ and ε on the cell face in direction $d\mathbf{r}_s$ by

$$\text{grad } \Phi = \frac{1}{h} (\Phi(\mathbf{r}_{ijk} + d\mathbf{r}_s) - \Phi(\mathbf{r}_{ijk})) \quad (15.24)$$

$$\varepsilon = \frac{1}{2} (\varepsilon(\mathbf{r}_{ijk} + d\mathbf{r}_s) + \varepsilon(\mathbf{r}_{ijk})) \quad (15.25)$$

and obtain the discrete equation

$$-Q_{ijk} = h \sum_{s=1}^6 \frac{\varepsilon(\mathbf{r}_{ijk} + d\mathbf{r}_s) + \varepsilon(\mathbf{r}_{ijk})}{2} (\Phi(\mathbf{r}_{ijk} + d\mathbf{r}_s) - \Phi(\mathbf{r}_{ijk})) \quad (15.26)$$

and finally the iteration

$$\Phi^{\text{new}}(\mathbf{r}_{ijk}) = \frac{\sum \frac{\varepsilon(\mathbf{r}_{ijk} + d\mathbf{r}_s) + \varepsilon(\mathbf{r}_{ijk})}{2} \Phi^{\text{old}}(\mathbf{r}_{ijk} + d\mathbf{r}_s) + \frac{Q_{ijk}}{h}}{\sum \frac{\varepsilon(\mathbf{r}_{ijk} + d\mathbf{r}_s) + \varepsilon(\mathbf{r}_{ijk})}{2}}. \quad (15.27)$$

15.1.4 Discontinuous ε

For practical applications, models are often used with piecewise constant ε . A simple example is the solvation of a charged molecule in a dielectric medium. Here $\varepsilon = \varepsilon_0$ within the molecule and $\varepsilon = \varepsilon_0 \varepsilon_1$ within the medium. At the boundary ε is discontinuous.

Equation (15.27) replaces the discontinuity by the average value $\varepsilon = \varepsilon_0(1 + \varepsilon_1)/2$ which can be understood as the discretization of a linear transition between the two values.

15.1.5 Solvation Energy of a Charged Sphere

We consider again a charged sphere, which is now embedded in a dielectric medium with relative dielectric constant ε_1 (Fig. 15.3).

For a spherically symmetrical problem (15.4) can be solved by application of Gauss's theorem

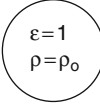
$$\begin{aligned} \varepsilon &= \varepsilon_1 \\ \rho &= 0 \end{aligned}$$


Fig. 15.3 Solution of a charged sphere in a dielectric medium

$$4\pi r^2 \varepsilon(r) \frac{d\Phi}{dr} = -4\pi \int \rho(r) r^2 dr = -q(r) \quad (15.28)$$

$$\Phi(r) = - \int_0^r \frac{q(r)}{4\pi r^2 \varepsilon(r)} + \Phi(0). \quad (15.29)$$

For the charged sphere we find

$$q(r) = \begin{cases} Qr^3/R^3 & \text{for } r < R \\ Q & \text{for } r > R \end{cases} \quad (15.30)$$

$$\Phi(r) = - \frac{Q}{4\pi \varepsilon_0 R^3} \frac{r^2}{2} + \Phi(0) \quad \text{for } r < R \quad (15.31)$$

$$\Phi(r) = - \frac{Q}{8\pi \varepsilon_0 R} + \Phi(0) + \frac{Q}{4\pi \varepsilon_0 \varepsilon_1} \left(\frac{1}{r} - \frac{1}{R} \right) \quad \text{for } r > R. \quad (15.32)$$

The constant $\Phi(0)$ is chosen to give vanishing potential at infinity

$$\Phi(0) = \frac{Q}{4\pi \varepsilon_0 \varepsilon_1 R} + \frac{Q}{8\pi \varepsilon_0 R}. \quad (15.33)$$

15.1.5.1 Numerical Results

The numerical results show systematic errors in the center of the sphere. These are mainly due to the discretization of the sphere (Fig. 15.4). The charge is distributed over a finite number N_C of grid cells and therefore the volume deviates from $4\pi R^3/3$. Defining an effective radius by

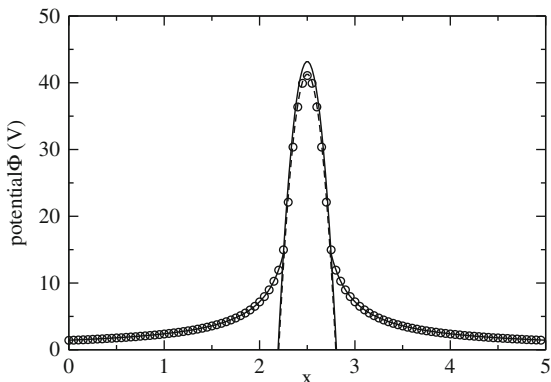
$$\frac{4\pi}{3} R_{\text{eff}}^3 = N_C h^3 \quad (15.34)$$

the deviation of the potential is

$$\Delta \Phi(0) = \frac{Q}{4\pi \varepsilon_0} \left(\frac{1}{\varepsilon_1} + \frac{1}{2} \right) \left(\frac{1}{R_{\text{eff}}} - \frac{1}{R} \right) \approx \frac{Q}{4\pi \varepsilon_0 R} \left(\frac{1}{\varepsilon_1} + \frac{1}{2} \right) \frac{R - R_{\text{eff}}}{R} \quad (15.35)$$

which for our numerical experiment amounts to 0.26 V.

Fig. 15.4 Charged sphere in a dielectric medium. Numerical results for $\epsilon_1 = 4$ outside the sphere (*circles*) are compared to the exact solution (15.31) and (15.32), *solid curves*). The *dashed line* shows the analytical result corrected for the error which is induced by the continuous transition of ϵ_1 (15.1.4)



15.1.6 The Shifted Grid Method

The error (Sect. 15.1.4) can be reduced by the following method. Consider a thin box with the normal vector \mathbf{A} parallel to the gradient of ϵ . Application of Gauss's theorem gives (Fig. 15.5)

$$\epsilon_+ \mathbf{A} \text{ grad } \Phi_+ = \epsilon_- \mathbf{A} \text{ grad } \Phi_- \tag{15.36}$$

The normal component of $\text{grad } \Phi$ changes by a factor of ϵ_+/ϵ_- . The discontinuity is located at the surface of a grid cell. Therefore it is of advantage to use a different grid for ϵ which is shifted by $h/2$ in all directions [77] (Figs. 15.6, 15.7, 15.8):

$$\epsilon_{ijk} = \epsilon \left(\left(i + \frac{1}{2} \right) h, \left(j + \frac{1}{2} \right) h, \left(k + \frac{1}{2} \right) h \right). \tag{15.37}$$

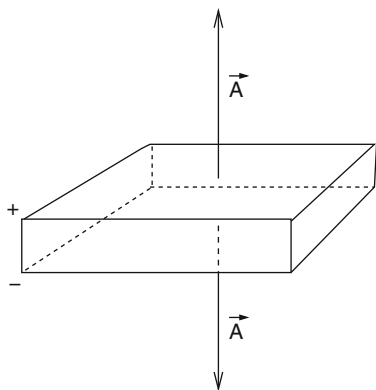


Fig. 15.5 Discontinuity in three dimensions

Fig. 15.6 Shifted grid method. A different grid is used for the discretization of ϵ which is shifted by $h/2$ in all directions

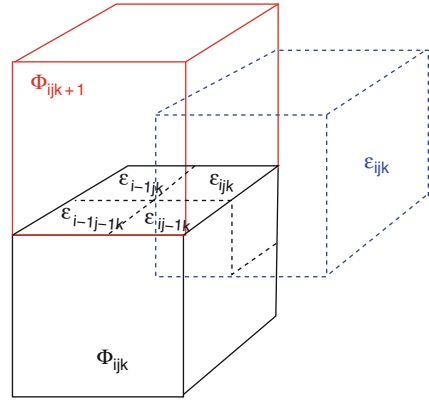


Fig. 15.7 Charged sphere with the shifted grid method. The numerically calculated potential for $\epsilon_1 = 4$ outside the sphere (circles) is compared to the exact solution ((15.31) and (15.32), solid curves)

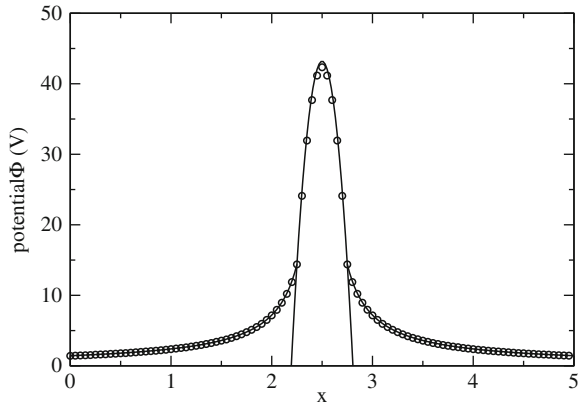
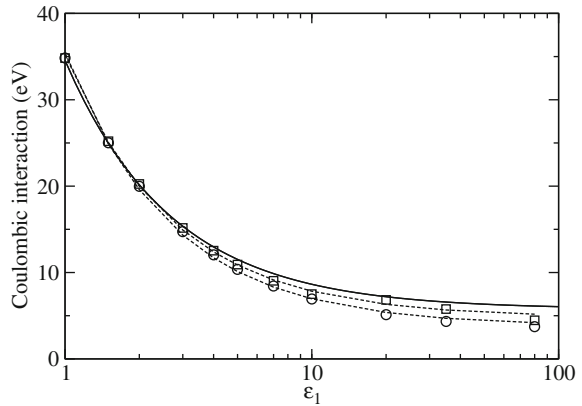


Fig. 15.8 Comparison of numerical errors. The Coulombic interaction of a charged sphere is calculated according to ((15.27), circles) and ((15.38), squares) and compared to the analytical solution (solid curve)



ε has to be averaged over four neighboring cells to give

$$(\varepsilon \mathbf{Agrad} \phi)_{ijk} = \frac{\phi_{i,j,k+1} - \phi_{i,j,k}}{h} \frac{\varepsilon_{ijk} + \varepsilon_{i,j-1,k} + \varepsilon_{i-1,j,k} + \varepsilon_{i-1,j-1,k}}{4} + \dots \quad (15.38)$$

15.2 Poisson Boltzmann Equation for an Electrolyte

Let us consider additional mobile charges (for instance, ions in an electrolyte). N_i denotes the average number of ions of type i with charge Q_i . The system is neutral if

$$\sum_i N_i Q_i = 0. \quad (15.39)$$

The interaction energy of a charge Q_i in the electrostatic potential Φ is

$$\Phi Q_i. \quad (15.40)$$

This interaction changes the ion numbers according to the Boltzmann factor:

$$N'_i = N_i e^{-Q_i \Phi / k_B T}. \quad (15.41)$$

The charge density of the free ions is

$$\rho_{\text{Ion}} = \sum_i N'_i Q_i = \sum_i N_i Q_i e^{-Q_i \Phi / k_B T} \quad (15.42)$$

which has to be taken into account in the Poisson equation. Combination gives the Poisson–Boltzmann equation [78–80]

$$\text{div}(\varepsilon \text{grad} \Phi) = - \sum_i N_i Q_i e^{-Q_i \Phi / k_B T} - \rho_{\text{fix}}. \quad (15.43)$$

For small ion concentrations the exponential can be expanded

$$e^{-Q_i \Phi / k_B T} \approx 1 - \frac{Q_i \Phi}{k_B T} + \frac{1}{2} \left(\frac{Q_i \Phi}{k_B T} \right)^2 + \dots \quad (15.44)$$

and the linearized Poisson–Boltzmann equation is obtained:

$$\text{div}(\varepsilon \text{grad} \Phi) = -\rho_{\text{fix}} + \sum_i \frac{N_i Q_i^2}{k_B T} \Phi. \quad (15.45)$$

With

$$\varepsilon = \varepsilon_0 \varepsilon_r \quad (15.46)$$

and the definition

$$\kappa^2 = \frac{1}{\varepsilon_0 \varepsilon_r k T} \sum N_i Q_i^2 = \frac{e^2}{\varepsilon_0 \varepsilon_r k T} \sum N_i Z_i^2 \quad (15.47)$$

we have finally

$$\operatorname{div}(\varepsilon_r \operatorname{grad} \Phi) - \varepsilon_r \kappa^2 \Phi = -\frac{1}{\varepsilon_0} \rho. \quad (15.48)$$

For a charged sphere with radius a embedded in a homogeneous medium the solution of (15.48) is given by

$$\Phi = \frac{A}{r} e^{-\kappa r} \quad A = \frac{e}{4\pi \varepsilon_0 \varepsilon_r} \frac{e^{\kappa a}}{1 + \kappa a}. \quad (15.49)$$

The potential is shielded by the ions. Its range is of the order $\lambda_{\text{Debye}} = 1/\kappa$ (the so-called Debye length).

15.2.1 Discretization of the Linearized Poisson–Boltzmann Equation

To solve (15.48) the discrete equation (15.26) is generalized to [81]

$$\begin{aligned} \sum \frac{\varepsilon_r(\mathbf{r}_{ijk} + d\mathbf{r}_s) + \varepsilon_r(\mathbf{r}_{ijk})}{2} (\Phi(\mathbf{r}_{ijk} + d\mathbf{r}_s) - \Phi(\mathbf{r}_{ijk})) \\ - \varepsilon_r(\mathbf{r}_{ijk}) \kappa^2 (\mathbf{r}_{ijk}) h^2 \Phi(\mathbf{r}_{ijk}) = -\frac{Q_{ijk}}{h \varepsilon_0}. \end{aligned} \quad (15.50)$$

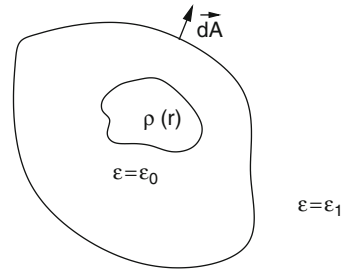
If ε is constant then we have to iterate

$$\Phi^{\text{new}}(\mathbf{r}_{ijk}) = \frac{Q_{ijk}}{h \varepsilon_0 \varepsilon_r} + \frac{\sum \Phi^{\text{old}}(\mathbf{r}_{ijk} + d\mathbf{r}_s)}{6 + h^2 \kappa^2 (\mathbf{r}_{ijk})}. \quad (15.51)$$

15.3 Boundary Element Method for the Poisson Equation

Often continuum models are used to describe the solvation of a subsystem which is treated with a high-accuracy method. The polarization of the surrounding solvent or protein is described by its dielectric constant ε and the subsystem is placed inside a cavity with $\varepsilon = \varepsilon_0$. Instead of solving the Poisson equation for a large solvent volume another kind of method is often used which replaces the polarization of the medium by a distribution of charges over the boundary surface.

Fig. 15.9 Cavity in a dielectric medium



In the following we consider model systems which are composed of two spatial regions (Fig. 15.9):

- the outer region is filled with a dielectric medium (ϵ_1) and contains no free charges
- the inner region (“Cavity”) contains a charge distribution $\rho(r)$ and its dielectric constant is $\epsilon = \epsilon_0$.

15.3.1 Integral Equations for the Potential

Starting from the Poisson equation

$$\text{div}(\epsilon(\mathbf{r})\text{grad } \Phi(\mathbf{r})) = -\rho(\mathbf{r}) \tag{15.52}$$

we will derive some useful integral equations in the following. First we apply Gauss’s theorem to the expression [82]

$$\begin{aligned} & \text{div} \left[G(\mathbf{r} - \mathbf{r}')\epsilon(\mathbf{r})\text{grad}(\Phi(\mathbf{r})) - \Phi(\mathbf{r})\epsilon(\mathbf{r})\text{grad}(G(\mathbf{r} - \mathbf{r}')) \right] \\ &= -\rho(\mathbf{r})G(\mathbf{r} - \mathbf{r}') - \Phi(\mathbf{r})\epsilon(\mathbf{r})\text{div grad}(G(\mathbf{r} - \mathbf{r}')) - \Phi(\mathbf{r})\text{grad}(\epsilon(\mathbf{r}))\text{grad}(G(\mathbf{r} - \mathbf{r}')) \end{aligned} \tag{15.53}$$

with the yet undetermined function $G(\mathbf{r} - \mathbf{r}')$. Integration over a volume V gives

$$\begin{aligned} & - \int_V dV \left(\rho(\mathbf{r})G(\mathbf{r} - \mathbf{r}') + \Phi(\mathbf{r})\epsilon(\mathbf{r})\text{div grad}(G(\mathbf{r} - \mathbf{r}')) \right. \\ & \quad \left. + \Phi(\mathbf{r})\text{grad}(\epsilon(\mathbf{r}))\text{grad}(G(\mathbf{r} - \mathbf{r}')) \right) \\ &= \oint_{(V)} dA \left(G(\mathbf{r} - \mathbf{r}')\epsilon(\mathbf{r})\frac{\partial}{\partial n}(\Phi(\mathbf{r})) - \Phi(\mathbf{r})\epsilon(\mathbf{r})\frac{\partial}{\partial n}(G(\mathbf{r} - \mathbf{r}')) \right). \end{aligned} \tag{15.54}$$

Now chose G as the fundamental solution of the Poisson equation

$$G_0(\mathbf{r} - \mathbf{r}') = -\frac{1}{4\pi|\mathbf{r} - \mathbf{r}'|} \tag{15.55}$$

which obeys

$$\operatorname{div} \operatorname{grad} G_0 = \delta(\mathbf{r} - \mathbf{r}') \quad (15.56)$$

to obtain the following integral equation for the potential:

$$\begin{aligned} \Phi(\mathbf{r}')\varepsilon(\mathbf{r}) &= \int dV \frac{\rho(\mathbf{r})}{4\pi|\mathbf{r} - \mathbf{r}'|} + \frac{1}{4\pi} \int dV \Phi(\mathbf{r}) \operatorname{grad}(\varepsilon(\mathbf{r})) \operatorname{grad} \left(\frac{1}{|\mathbf{r} - \mathbf{r}'|} \right) \\ &- \frac{1}{4\pi} \oint_{(V)} dA \left(\frac{1}{|\mathbf{r} - \mathbf{r}'|} \varepsilon(\mathbf{r}) \frac{\partial}{\partial n} (\Phi(\mathbf{r})) + \Phi(\mathbf{r}) \varepsilon(\mathbf{r}) \frac{\partial}{\partial n} \left(\frac{1}{|\mathbf{r} - \mathbf{r}'|} \right) \right) \end{aligned} \quad (15.57)$$

First consider as the integration volume a sphere with increasing radius. Then the surface integral vanishes for infinite radius ($\Phi \rightarrow 0$ at large distances) [82] (Fig. 15.10).

The gradient of $\varepsilon(\mathbf{r})$ is nonzero only on the boundary surface of the cavity and with the limiting procedure ($d \rightarrow 0$)

$$\operatorname{grad}(\varepsilon(\mathbf{r}))dV = \mathbf{n} \frac{\varepsilon_1 - 1}{d} \varepsilon_0 dV = dA \mathbf{n}(\varepsilon_1 - 1)\varepsilon_0 \quad (15.58)$$

we obtain

$$\Phi(\mathbf{r}') = \frac{1}{\varepsilon(\mathbf{r}')} \int_{\text{cav}} dV \frac{\rho(\mathbf{r})}{4\pi|\mathbf{r} - \mathbf{r}'|} + \frac{(\varepsilon_1 - 1)\varepsilon_0}{4\pi\varepsilon(\mathbf{r}')} \oint_S dA \Phi(\mathbf{r}) \frac{\partial}{\partial n} \frac{1}{|\mathbf{r} - \mathbf{r}'|}. \quad (15.59)$$

This equation allows to calculate the potential inside and outside the cavity from the given charge density and the potential at the boundary.

Next we apply (15.57) to the cavity volume (where $\varepsilon = \varepsilon_0$) and obtain

$$\begin{aligned} \Phi_{\text{in}}(\mathbf{r}') &= \int_V dV \frac{\rho(\mathbf{r})}{4\pi|\mathbf{r} - \mathbf{r}'|\varepsilon_0} \\ &- \frac{1}{4\pi} \oint_{(V)} dA \left(\Phi_{\text{in}}(\mathbf{r}) \frac{\partial}{\partial n} \frac{1}{|\mathbf{r} - \mathbf{r}'|} - \frac{1}{|\mathbf{r} - \mathbf{r}'|} \frac{\partial}{\partial n} \Phi_{\text{in}}(\mathbf{r}) \right). \end{aligned} \quad (15.60)$$

From comparison with (15.59) we have

$$\oint dA \frac{1}{|\mathbf{r} - \mathbf{r}'|} \frac{\partial}{\partial n} \Phi_{\text{in}}(\mathbf{r}) = \varepsilon_1 \oint dA \Phi_{\text{in}}(\mathbf{r}) \frac{\partial}{\partial n} \frac{1}{|\mathbf{r} - \mathbf{r}'|} \quad (15.61)$$

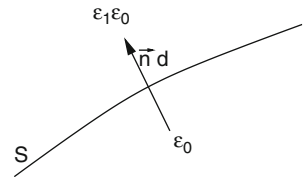


Fig. 15.10 Discontinuity at the cavity boundary

and the potential can be alternatively calculated from the values of its normal gradient at the boundary

$$\Phi(\mathbf{r}') = \frac{1}{\varepsilon(\mathbf{r}')} \int_{\text{cav}} dV \frac{\rho(\mathbf{r})}{4\pi|\mathbf{r}-\mathbf{r}'|} + \frac{(1-\frac{1}{\varepsilon_1})\varepsilon_0}{4\pi\varepsilon(\mathbf{r}')} \oint_S dA \frac{1}{|\mathbf{r}-\mathbf{r}'|} \frac{\partial}{\partial n} \Phi_{\text{in}}(\mathbf{r}). \quad (15.62)$$

This equation can be interpreted as the potential generated by the charge density ρ plus an additional surface charge density

$$\sigma(\mathbf{r}) = \left(1 - \frac{1}{\varepsilon_1}\right) \varepsilon_0 \frac{\partial}{\partial n} \Phi_{\text{in}}(\mathbf{r}). \quad (15.63)$$

Integration over the volume outside the cavity (where $\varepsilon = \varepsilon_1\varepsilon_0$) gives the following expression for the potential:

$$\Phi_{\text{out}}(\mathbf{r}') = \frac{1}{4\pi} \oint_{(V)} dA \left(\Phi_{\text{out}}(\mathbf{r}) \frac{\partial}{\partial n} \frac{1}{|\mathbf{r}-\mathbf{r}'|} - \frac{1}{|\mathbf{r}-\mathbf{r}'|} \frac{\partial}{\partial n} \Phi_{\text{out}}(\mathbf{r}) \right). \quad (15.64)$$

At the boundary the potential is continuous

$$\Phi_{\text{out}}(\mathbf{r}) = \Phi_{\text{in}}(\mathbf{r}) \quad \mathbf{r} \in A, \quad (15.65)$$

whereas the normal derivative (hence the normal component of the electric field) has a discontinuity

$$\varepsilon_1 \frac{\partial \Phi_{\text{out}}}{\partial n} = \frac{\partial \Phi_{\text{in}}}{\partial n}. \quad (15.66)$$

15.3.2 Calculation of the Boundary Potential

For a numerical treatment the boundary surface is approximated by a finite set of small surface elements $S_i, i = 1 \dots N$ centered at \mathbf{r}_i with an area A_i and normal vector \mathbf{n}_i . (We assume planar elements in the following, the curvature leads to higher order corrections) (Fig. 15.11).

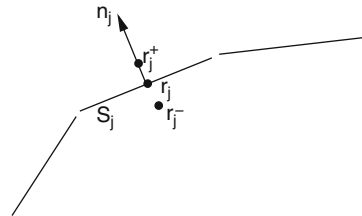


Fig. 15.11 Representation of the boundary by surface elements

The corresponding values of the potential and its normal derivative are denoted as $\Phi_i = \Phi(\mathbf{r}_i)$ and $\frac{\partial \Phi_i}{\partial n} = \mathbf{n}_i \text{grad } \Phi(\mathbf{r}_i)$. At a point \mathbf{r}_j^\pm close to the element S_j we obtain the following approximate equations:

$$\Phi_{\text{in}}(\mathbf{r}_j^-) = \int_V dV \frac{\rho(\mathbf{r})}{4\pi |\mathbf{r} - \mathbf{r}_j^-| \epsilon_0} - \frac{1}{4\pi} \sum_i \Phi_i \oint_{S_i} dA \frac{\partial}{\partial n} \frac{1}{|\mathbf{r} - \mathbf{r}_j^-|} + \frac{1}{4\pi} \sum_i \frac{\partial \Phi_{i,\text{in}}}{\partial n} \oint_{S_i} dA \frac{1}{|\mathbf{r} - \mathbf{r}_j^-|} \quad (15.67)$$

$$\Phi_{\text{out}}(\mathbf{r}_j^+) = \frac{1}{4\pi} \sum_i \Phi_i \oint_{S_i} dA \frac{\partial}{\partial n} \frac{1}{|\mathbf{r} - \mathbf{r}_j^+|} - \frac{1}{4\pi} \sum_i \frac{\partial \Phi_{i,\text{out}}}{\partial n} \oint_{S_i} dA \frac{1}{|\mathbf{r} - \mathbf{r}_j^+|}. \quad (15.68)$$

These two equations can be combined to obtain a system of equations for the potential values only. To that end we approach the boundary symmetrically with $\mathbf{r}_i^\pm = \mathbf{r}_i \pm d\mathbf{n}_i$. Under this circumstance

$$\begin{aligned} \oint_{S_i} dA \frac{1}{|\mathbf{r} - \mathbf{r}_j^+|} &= \oint_{S_i} dA \frac{1}{|\mathbf{r} - \mathbf{r}_j^-|} \\ \oint_{S_i} dA \frac{\partial}{\partial n} \frac{1}{|\mathbf{r} - \mathbf{r}_i^+|} &= - \oint_{S_i} dA \frac{\partial}{\partial n} \frac{1}{|\mathbf{r} - \mathbf{r}_i^-|} \\ \oint_{S_i} dA \frac{\partial}{\partial n} \frac{1}{|\mathbf{r} - \mathbf{r}_j^+|} &= \oint_{S_i} dA \frac{\partial}{\partial n} \frac{1}{|\mathbf{r} - \mathbf{r}_j^-|} \quad j \neq i \end{aligned} \quad (15.69)$$

and we find

$$\begin{aligned} (1 + \epsilon_1)\Phi_j &= \int_V dV \frac{\rho(\mathbf{r})}{4\pi \epsilon_0 |\mathbf{r} - \mathbf{r}_j|} - \frac{1}{4\pi} \sum_{i \neq j} (1 - \epsilon_1)\Phi_i \oint_{S_i} dA \frac{\partial}{\partial n} \frac{1}{|\mathbf{r} - \mathbf{r}_j^-|} - \frac{1}{4\pi} (1 + \epsilon_1)\Phi_j \oint_{S_j} dA \frac{\partial}{\partial n} \frac{1}{|\mathbf{r} - \mathbf{r}_j^-|}. \end{aligned} \quad (15.70)$$

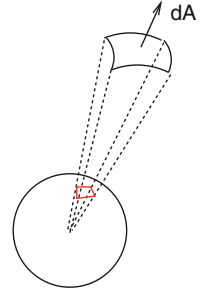
The integrals for $i \neq j$ can be approximated by

$$\oint_{S_i} dA \frac{\partial}{\partial n} \frac{1}{|\mathbf{r} - \mathbf{r}_j^-|} = A_i \mathbf{n}_i \text{grad}_i \frac{1}{|\mathbf{r}_i - \mathbf{r}_j|}. \quad (15.71)$$

The second integral has a simple geometrical interpretation (Fig. 15.12).

Since $\text{grad} \frac{1}{|r-r'|} = -\frac{1}{|r-r'|^2} \frac{r-r'}{|r-r'|}$ the area element dA is projected onto a sphere with unit radius. The integral $\oint_{S_j} dA \text{grad}_{r-} \frac{1}{|\mathbf{r}_j - \mathbf{r}_j^-|}$ is given by the solid angle of \mathbf{S}_j with respect to r' . For $r' \rightarrow r_j$ from inside this is just minus half of the full space angle of 4π . Thus we have

Fig. 15.12 Projection of the surface element



$$(1 + \epsilon_1)\Phi_j = \int_V dV \frac{\rho(\mathbf{r})}{4\pi|\mathbf{r} - \mathbf{r}_j|^{\epsilon_0}} - \frac{1}{4\pi} \sum_{i \neq j} (1 - \epsilon_1)\Phi_i A_i \frac{\partial}{\partial n_i} \frac{1}{|\mathbf{r}_i - \mathbf{r}_j|} + \frac{1}{2}(1 + \epsilon_1)\Phi_j \quad (15.72)$$

or

$$\Phi_j = \frac{2}{1 + \epsilon_1} \int_V dV \frac{\rho(\mathbf{r})}{4\pi\epsilon_0|\mathbf{r} - \mathbf{r}_j|} + \frac{1}{2\pi} \sum_{i \neq j} \frac{\epsilon_1 - 1}{\epsilon_1 + 1} \Phi_i A_i \frac{\partial}{\partial n_i} \frac{1}{|\mathbf{r}_i - \mathbf{r}_j|}. \quad (15.73)$$

This system of equations can be used to calculate the potential on the boundary. The potential inside the cavity is then given by (15.59). Numerical stability is improved by a related method which considers the potential gradient along the boundary. Taking the normal derivative

$$\frac{\partial}{\partial n_j} = \mathbf{n}_j \text{grad}_{r_j \pm} \quad (15.74)$$

of (15.67, 15.68) gives

$$\begin{aligned} \frac{\partial}{\partial n_j} \Phi_{\text{in}}(\mathbf{r}_j^-) &= \frac{\partial}{\partial n_j} \int_V dV \frac{\rho(\mathbf{r})}{4\pi|\mathbf{r} - \mathbf{r}_j^-|^{\epsilon_0}} \\ &- \frac{1}{4\pi} \sum_i \Phi_i \oint_{S_i} dA \frac{\partial^2}{\partial n \partial n_j} \frac{1}{|\mathbf{r} - \mathbf{r}_j^-|} + \frac{1}{4\pi} \sum_i \frac{\partial \Phi_{i,\text{in}}}{\partial n} \oint_{S_i} dA \frac{\partial}{\partial n_j} \frac{1}{|\mathbf{r} - \mathbf{r}_j^-|} \end{aligned} \quad (15.75)$$

$$\begin{aligned} \frac{\partial}{\partial n_j} \Phi_{\text{out}}(\mathbf{r}_j^+) &= \frac{1}{4\pi} \sum_i \Phi_i \oint_{S_i} dA \frac{\partial^2}{\partial n \partial n_j} \frac{1}{|\mathbf{r} - \mathbf{r}_j^+|} \\ &- \frac{1}{4\pi} \sum_i \frac{\partial \Phi_{i,\text{out}}}{\partial n} \oint_{S_i} dA \frac{\partial}{\partial n_j} \frac{1}{|\mathbf{r} - \mathbf{r}_j^+|}. \end{aligned} \quad (15.76)$$

In addition to (15.69) we have now

$$\oint_{S_i} dA \frac{\partial^2}{\partial n \partial n_j} \frac{1}{|\mathbf{r} - \mathbf{r}_j^-|} = \oint_{S_i} dA \frac{\partial^2}{\partial n \partial n_j} \frac{1}{|\mathbf{r} - \mathbf{r}_j^+|} \quad (15.77)$$

and the sum of the two equations gives

$$\begin{aligned} & \left(1 + \frac{1}{\epsilon_1}\right) \frac{\partial}{\partial n_j} \Phi_{\text{in},j} \\ &= \frac{\partial}{\partial n_j} \left(\int_V dV \frac{\rho(\mathbf{r})}{4\pi\epsilon_0|\mathbf{r}-\mathbf{r}_j|} + \frac{1-\frac{1}{\epsilon_1}}{4\pi} \sum_{i \neq j} A_i \frac{\partial \Phi_{i,\text{in}}}{\partial n} \frac{1}{|\mathbf{r}_i-\mathbf{r}_j|} \right) \\ &+ \frac{1+\frac{1}{\epsilon_1}}{2\pi} \frac{\partial \Phi_{j,\text{in}}}{\partial n} \end{aligned} \quad (15.78)$$

or finally

$$\begin{aligned} \frac{\partial}{\partial n_j} \Phi_{\text{in},j} &= \frac{2\epsilon_1}{\epsilon_1+1} \frac{\partial}{\partial n_j} \int_V dV \frac{\rho(\mathbf{r})}{4\pi\epsilon_0|\mathbf{r}-\mathbf{r}_j|} \\ &+ 2 \frac{\epsilon_1-1}{\epsilon_1+1} \sum_{i \neq j} A_i \frac{\partial \Phi_{i,\text{in}}}{\partial n} \frac{\partial}{\partial n_j} \frac{1}{|\mathbf{r}_i-\mathbf{r}_j|}. \end{aligned} \quad (15.79)$$

In terms of the surface charge density this reads:

$$\sigma'_j = 2\epsilon_0 \frac{(1-\epsilon_1)}{(1+\epsilon_1)} \left(-\mathbf{n}_j \text{grad} \int dV \frac{\rho(\mathbf{r})}{4\pi\epsilon_0|\mathbf{r}-\mathbf{r}'|} + \frac{1}{4\pi\epsilon_0} \sum_{i \neq j} \sigma'_i A_i \frac{\mathbf{n}_j(\mathbf{r}_j-\mathbf{r}_i)}{|\mathbf{r}_i-\mathbf{r}_j|^3} \right). \quad (15.80)$$

This system of linear equations can be solved directly or iteratively (a simple damping scheme $\sigma'_m \rightarrow \omega\sigma'_m + (1-\omega)\sigma'_{m,\text{old}}$ with $\omega \approx 0.6$ helps to get rid of oscillations). From the surface charges $\sigma_i A_i$ the potential is obtained with the help of (15.62).

15.4 Boundary Element Method for the Linearized Poisson–Boltzmann Equation

We consider now a cavity within an electrolyte. The fundamental solution of the linear Poisson–Boltzmann equation (15.48)

$$G_\kappa(\mathbf{r}-\mathbf{r}') = -\frac{e^{-\kappa|\mathbf{r}-\mathbf{r}'|}}{4\pi|\mathbf{r}-\mathbf{r}'|} \quad (15.81)$$

obeys

$$\text{div grad } G_\kappa(\mathbf{r}-\mathbf{r}') - \kappa^2 G_\kappa(\mathbf{r}-\mathbf{r}') = \delta(\mathbf{r}-\mathbf{r}'). \quad (15.82)$$

Inserting into Green's theorem (15.54) we obtain the potential outside the cavity

$$\Phi_{\text{out}}(\mathbf{r}') = - \oint_{(V)} dA \left(\Phi_{\text{out}}(\mathbf{r}) \frac{\partial}{\partial n} G_{\kappa}(\mathbf{r} - \mathbf{r}') - G_{\kappa}(\mathbf{r} - \mathbf{r}') \frac{\partial}{\partial n} \Phi_{\text{out}}(\mathbf{r}) \right) \quad (15.83)$$

which can be combined with (15.60, 15.66) to give the following equations [83]

$$(1 + \epsilon_1)\Phi(\mathbf{r}') = \oint dA \left[\Phi(\mathbf{r}) \frac{\partial}{\partial n} (G_0 - \epsilon_1 G_{\kappa}) - (G_0 - G_{\kappa}) \frac{\partial}{\partial n} \Phi_{\text{in}}(\mathbf{r}) \right] + \int \frac{\rho(\mathbf{r})}{4\pi\epsilon_0|\mathbf{r} - \mathbf{r}'|} dV \quad (15.84)$$

$$(1 + \epsilon_1) \frac{\partial}{\partial n'} \Phi_{\text{in}}(\mathbf{r}') = \oint dA \Phi(\mathbf{r}) \frac{\partial^2}{\partial n \partial n'} (G_0 - G_{\kappa}) - \oint dA \frac{\partial}{\partial n} \Phi_{\text{in}}(\mathbf{r}) \frac{\partial}{\partial n'} \left(G_0 - \frac{1}{\epsilon_1} G_{\kappa} \right) + \frac{\partial}{\partial n'} \int \frac{\rho(\mathbf{r})}{4\pi\epsilon|\mathbf{r} - \mathbf{r}'|} dV. \quad (15.85)$$

For a set of discrete boundary elements the following equations determine the values of the potential and its normal derivative at the boundary:

$$\frac{1 + \epsilon_1}{2} \Phi_j = \sum_{i \neq j} \Phi_i \oint dA \frac{\partial}{\partial n} (G_0 - \epsilon_1 G_{\kappa}) - \sum_{i \neq j} \frac{\partial}{\partial n} \Phi_{i,\text{in}} \oint dA (G_0 - G_{\kappa}) + \int \frac{\rho(\mathbf{r})}{4\pi\epsilon_0|\mathbf{r} - \mathbf{r}_i|} dV \quad (15.86)$$

$$\frac{1 + \epsilon_1}{2} \frac{\partial}{\partial n'} \Phi_{i,\text{in}} = \sum_{i \neq j} \Phi_i \oint dA \frac{\partial^2}{\partial n \partial n'} (G_0 - G_{\kappa}) - \sum_{i \neq j} \frac{\partial}{\partial n} \Phi_{i,\text{in}} \oint dA \frac{\partial}{\partial n'} \left(G_0 - \frac{1}{\epsilon_1} G_{\kappa} \right) + \frac{\partial}{\partial n'} \int \frac{\rho(\mathbf{r})}{4\pi\epsilon|\mathbf{r} - \mathbf{r}_i|} dV. \quad (15.87)$$

The situation is much more involved than for the simpler Poisson equation (with $\kappa = 0$) since the calculation of a large number of integrals including such with singularities is necessary [83, 84].

15.5 Electrostatic Interaction Energy (Onsager Model)

A very important quantity in molecular physics is the electrostatic interaction of a molecule and the surrounding solvent [85, 86]. We calculate it by taking a small part of the charge distribution from infinite distance ($\Phi(r \rightarrow \infty) = 0$) into the cavity. The charge distribution thereby changes from $\lambda\rho(r)$ to $(\lambda + d\lambda)\rho(r)$ with $0 \leq \lambda \leq 1$. The corresponding energy change is

$$\begin{aligned}
 dE &= \int d\lambda \rho(r) \Phi_\lambda(r) dV \\
 &= \int d\lambda \rho(r) \left(\sum_n \frac{\sigma_n(\lambda) A_n}{4\pi \varepsilon_0 |\mathbf{r} - \mathbf{r}_n|} + \int \frac{\lambda \rho(r')}{4\pi \varepsilon_0 |\mathbf{r} - r'|} dV' \right) dV. \quad (15.88)
 \end{aligned}$$

Multiplication of (15.80) by a factor of λ shows that the surface charges $\lambda \sigma_n$ are the solution corresponding to the charge density $\lambda \rho(r)$. It follows that $\sigma_n(\lambda) = \lambda \sigma_n$ and hence

$$dE = \lambda d\lambda \int \rho(r) \left(\sum_n \frac{\sigma_n A_n}{4\pi \varepsilon_0 |\mathbf{r} - \mathbf{r}_n|} + \frac{\rho(r')}{4\pi \varepsilon_0 |\mathbf{r} - r'|} dV' \right). \quad (15.89)$$

The second summand is the self-energy of the charge distribution which does not depend on the medium. The first summand vanishes without a polarizable medium and gives the interaction energy. Hence we have the final expression

$$\begin{aligned}
 E_{\text{int}} &= \int dE = \int_0^1 \lambda d\lambda \int \rho(r) \sum_n \frac{\sigma_n A_n}{4\pi \varepsilon_0 |\mathbf{r} - \mathbf{r}_n|} dV \\
 &= \sum_n \sigma_n A_n \int \frac{\rho(r)}{8\pi \varepsilon_0 |\mathbf{r} - \mathbf{r}_n|} dV. \quad (15.90)
 \end{aligned}$$

For the special case of a spherical cavity with radius a an analytical solution by multipole expansion is available [87]

$$E_{\text{int}} = -\frac{1}{8\pi \varepsilon_0} \sum_l \sum_{m=-l}^l \frac{(l+1)(\varepsilon_1 - 1)}{[l + \varepsilon_1(l+1)]} a^{2l+1} M_l^m M_l^m \quad (15.91)$$

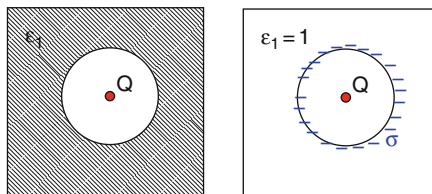
with the multipole moments

$$M_l^m = \int \rho(r, \theta, \varphi) \sqrt{\frac{4\pi}{2l+1}} r^l Y_l^m(\theta, \varphi) dV. \quad (15.92)$$

The first two terms of this series are

$$E_{\text{int}}^{(0)} = -\frac{1}{8\pi \varepsilon_0} \frac{\varepsilon_1 - 1}{\varepsilon_1 a} M_0^0 M_0^0 = -\frac{1}{8\pi \varepsilon_0} \left(1 - \frac{1}{\varepsilon_1}\right) \frac{Q^2}{a} \quad (15.93)$$

$$\begin{aligned}
 E_{\text{int}}^{(1)} &= -\frac{1}{8\pi \varepsilon_0} \frac{2(\varepsilon_1 - 1)}{(1 + 2\varepsilon_1)a^3} (M_1^{-1} M_1^{-1} + M_1^0 M_1^0 + M_1^1 M_1^1) \\
 &= -\frac{1}{8\pi \varepsilon_0} \frac{2(\varepsilon_1 - 1)}{1 + 2\varepsilon_1} \frac{\mu^2}{a^3}. \quad (15.94)
 \end{aligned}$$

Fig. 15.13 Surface charges

15.5.1 Example: Point Charge in a Spherical Cavity

Consider a point charge Q in the center of a spherical cavity of radius R . The dielectric constant is given by

$$\varepsilon = \begin{cases} \varepsilon_0 & r < R \\ \varepsilon_1 \varepsilon_0 & r > R \end{cases} . \quad (15.95)$$

Electric field and potential are inside the cavity

$$E = \frac{Q}{4\pi \varepsilon_0 r^2} \quad \Phi = \frac{Q}{4\pi \varepsilon_0 r} + \frac{Q}{4\pi \varepsilon_0 R} \left(\frac{1}{\varepsilon_1} - 1 \right) \quad (15.96)$$

and outside

$$E = \frac{Q}{4\pi \varepsilon_1 \varepsilon_0 r^2} \quad \Phi = \frac{Q}{4\pi \varepsilon_1 \varepsilon_0 r} \quad r > R \quad (15.97)$$

which in terms of the surface charge density σ is

$$E = \frac{Q + 4\pi R^2 \sigma}{4\pi \varepsilon_0 r^2} \quad r > R \quad (15.98)$$

with the total surface charge

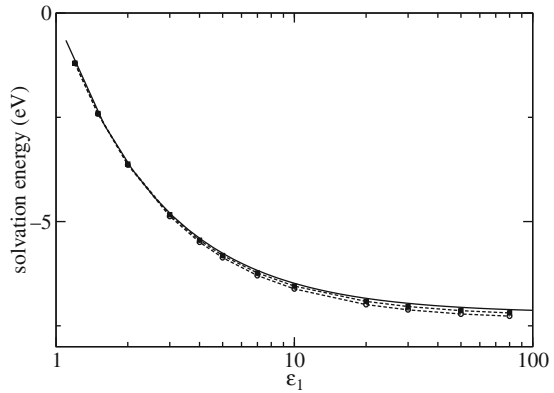
$$4\pi R^2 \sigma = Q \left(\frac{1}{\varepsilon_1} - 1 \right) . \quad (15.99)$$

The solvation energy (15.90) is given by

$$E_{\text{int}} = \frac{Q^2}{8\pi \varepsilon_0} \left(\frac{1}{\varepsilon_1} - 1 \right) \quad (15.100)$$

which is the first term (15.93) of the multipole expansion.

Fig. 15.14 Solvation energy with the boundary element method. A spherical cavity is simulated with a radius $a = 1 \text{ \AA}$ which contains a point charge in its center. The solvation energy is calculated with 25×25 (circles) and 50×50 (squares) surface elements of equal size. The exact expression (15.93) is shown by the solid curve



Problems

Problem 15.1 Linearized Poisson–Boltzmann Equation

This computer experiment simulates a homogeneously charged sphere in a dielectric medium. The electrostatic potential is calculated from the linearized Poisson–Boltzmann equation (15.50) on a cubic grid of up to 100^3 points. The potential $\Phi(x)$ is shown along a line through the center together with a log–log plot of the maximum change per iteration

$$|\Phi^{(n+1)}(\mathbf{r}) - \Phi^{(n)}(\mathbf{r})|$$

as a measure of convergence (Fig. 15.15).

Explore the dependence of convergence on

- the initial values which can be chosen either $\Phi(\mathbf{r}) = 0$ or from the analytical solution

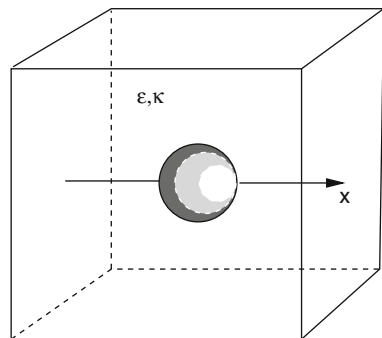


Fig. 15.15 Charged sphere in a dielectric medium

$$\Phi(\mathbf{r}) = \begin{cases} \frac{Q}{8\pi\epsilon_0 a} \frac{2+\epsilon(1+\kappa a)}{1+\kappa a} - \frac{Q}{8\pi\epsilon_0 a^3} r^2 & \text{for } r < a \\ \frac{Q e^{-\kappa(r-a)}}{4\pi\epsilon_0 \epsilon(\kappa a+1)r} & \text{for } r > a \end{cases}$$

- the relaxation parameter ω for different combinations of ϵ and κ
- the resolution of the grid

Problem 15.2 Boundary Element Method

In this computer element the solvation energy of a point charge within a spherical cavity is calculated with the boundary element method (15.80) (Fig. 15.16).

The calculated solvation energy is compared to the analytical value from (15.91)

$$E_{\text{solv}} = \frac{Q^2}{8\pi\epsilon_0 R} \sum_{n=1}^{\infty} \frac{s^{2n}}{R^{2n}} \frac{(\epsilon_1 - \epsilon_2)(n+1)}{n\epsilon_1 + (n+1)\epsilon_2} \tag{15.101}$$

where R is the cavity radius and s is the distance of the charge from the center of the cavity.

Explore the dependence of accuracy and convergence on

- the damping parameter ω
- the number of surface elements ($6 \times 6 \dots 42 \times 42$) which can be chosen either as $d\phi d\theta$ or $d\phi d \cos \theta$ (equal areas)
- the position of the charge.

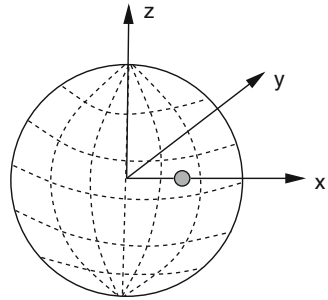


Fig. 15.16 Point charge inside a spherical cavity